

Orbital order of spinless fermions near an optical Feshbach resonance

Philipp Hauke,^{1,2,*} Erhai Zhao,^{3,2} Kritika Goyal^{†,4} Ivan H. Deutsch,⁴ W. Vincent Liu,^{5,2} and Maciej Lewenstein^{1,6,2}

¹*ICFO – Institut de Ciències Fotòniques, Parc Mediterrani de la Tecnologia, 08860 Castelldefels, Spain*

²*Kavli Institute for Theoretical Physics, University of California, Santa Barbara, CA 93106*

³*Department of Physics and Astronomy, George Mason University, Fairfax, VA 22030*

⁴*Center for Quantum Information and Control (CQuIC),*

and Department of Physics and Astronomy, University of New Mexico, Albuquerque NM 87131

⁵*Department of Physics and Astronomy, University of Pittsburgh, Pittsburgh, PA 15260*

⁶*ICREA – Institució Catalana de Recerca i Estudis Avançats, Lluís Companys 23, E-08010 Barcelona, Spain*

(Dated: July 30, 2021)

We study the quantum phases of a three-color Hubbard model that arises in the dynamics of the p -band orbitals of spinless fermions in an optical lattice. Strong, color-dependent interactions are induced by an optical Feshbach resonance. Starting from the microscopic scattering properties of ultracold atoms, we derive the orbital exchange constants at $1/3$ filling on the cubic optical lattice. Using this, we compute the phase diagram in a Gutzwiller ansatz. We find novel phases with ‘axial orbital order’ in which p_z and $p_x + ip_y$ (or $p_x - ip_y$) orbitals alternate.

PACS numbers: 03.75.Ss, 05.30.Fk, 67.85.-d, 71.10.Fd

Orbital physics of electrons plays an important role in strongly-correlated solid-state systems, *e.g.*, transition-metal oxides (see, *e.g.*, [1, 2] and references therein). In particular, intriguing quantum phases emerge due to the coupling of the orbital degree of freedom to the charge, spin, or lattice degrees of freedom [3, 4]. Such coupling, while leading to interesting effects, also complicates the theoretical treatment. It is, therefore, desirable to study simpler systems with the orbital degree of freedom decoupled from all others. Ultracold atoms in higher bands of optical lattices provide an ideal tool to study orbital dynamics in a well-controlled environment, including orbital-only models of single-species (spinless) fermions.

Several groups have now achieved loading and manipulating ultracold atoms in higher (such as p -) bands of optical lattices [5–9]. Techniques such as lattice ramping or radio-frequency pulses have been used to transfer atoms from the s - to higher bands, where they can stay in a metastable state for a sufficiently long time. For spinless fermionic atoms, the p -band can also be simply populated by first completely filling the s -band, requiring larger particle numbers, but less experimental control. To avoid undesired collisions between ground and excited-band atoms, the s -band atoms may be removed afterwards using laser pulses [10].

The interaction between fermionic atoms is usually weak at low temperatures because the Pauli exclusion principle only allows scattering in high partial-wave channels (p , f , *etc.*). One way to increase the p -wave elastic scattering cross section is to employ a Feshbach resonance (FR) [11]. Typically, this is done by coupling channels in the electronic ground state through magnetic fields. For

the case of p -waves, however, this method usually leads to significant atom losses through three-body inelastic collisions because the scattering state is well localized by the angular momentum barrier, and has good Franck-Condon overlap with more deeply bound molecules [12]. To circumvent this problem, recently Ref. [13] considered enhanced p -wave interactions via an optical FR (OFR) between a scattering state and an electronically excited “purely-long-range” molecule. Such molecules have inner turning points at very large distances (*e.g.*, $> 50a_0$ in ^{171}Yb), well beyond the chemical binding region, and thus three-body recombination should be highly suppressed. This approach not only allows to study strongly-correlated phases, but also provides for a high degree of control. In particular, the interaction strength among different p -orbitals can be tuned differently.

Motivated by these developments, we investigate in this article the phase diagram of spinless fermions on a cubic lattice near an OFR described by the following Hubbard-like model:

$$H = - \sum_{\mathbf{i}, \mu, \nu} t_{\mu, \nu} (c_{\mu, \mathbf{i}}^\dagger c_{\mu, \mathbf{i} + \mathbf{e}_\nu} + h.c.) + \sum_{\mathbf{i}} [V_1 n_{x, \mathbf{i}} n_{y, \mathbf{i}} + V_2 (n_{x, \mathbf{i}} n_{z, \mathbf{i}} + n_{y, \mathbf{i}} n_{z, \mathbf{i}}) + (iV_3 c_{x, \mathbf{i}}^\dagger c_{y, \mathbf{i}} n_{z, \mathbf{i}} + h.c.)]. \quad (1)$$

The operator $c_{\mu, \mathbf{i}}$ destroys a fermion in the orbital p_μ at site \mathbf{i} , and $n_{\mu, \mathbf{i}}$ is the corresponding number operator. The lattice spacing is set to 1, \mathbf{e}_ν is the unit vector in direction ν , and $\mu, \nu = x, y, z$. The nearest-neighbor hopping amplitude $t_{\mu, \nu}$ describes hopping of fermions in orbital p_μ along the direction \mathbf{e}_ν . Due to the anisotropy of the p -orbital Wannier wave functions, it is direction and orbital dependent [14–16], $t_{\mu, \nu} = t_{\parallel} \delta_{\mu, \nu} + t_{\perp} (1 - \delta_{\mu, \nu})$.

The interactions $V_{1,2,3}$ are induced by an OFR laser [13] which couples the electronic ground state of the atom to an excited state. The interaction can be expressed in terms of the (p -wave) pseudo-potential V_p^m for two particles with mass M and relative an-

[†]K. G. previously published under the name K. Kanjilal.

*Electronic address: philipp.hauke@icfo.es

gular momentum m , $V_p^m(\mathbf{r}) = \lim_{s \rightarrow 0} \frac{3R}{2M} \frac{\delta(r-s)}{s^3} \partial_r^3 r^2$. The real part of the p -wave scattering volume, $R = \text{Re}[(a_p^m)^3]$, can be tuned by the detuning and the intensity of the OFR laser. Expanding field operators in the Wannier basis, $\psi(\mathbf{r}) = \sum_{\mathbf{i}, \mu} w_\mu(\mathbf{r} - \mathbf{i}) c_{\mu, \mathbf{i}}$, the interaction term $\int d^3 r_1 \int d^3 r_2 \psi^\dagger(\mathbf{r}_1) \psi^\dagger(\mathbf{r}_2) V_p^m(\mathbf{r}_1 - \mathbf{r}_2) \psi(\mathbf{r}_1) \psi(\mathbf{r}_2)$ leads to the on-site, inter-orbital interaction $H_{\text{int}} = \sum_{\mathbf{i}} V_{\mu, \nu, \mu', \nu'} c_{\mu, \mathbf{i}}^\dagger c_{\nu', \mathbf{i}}^\dagger c_{\nu, \mathbf{i}} c_{\mu, \mathbf{i}}$, where repeated indices are summed over. (We neglect all off-site interactions.) The matrix element $V_{\mu, \nu, \mu', \nu'} = \sum_m \int d^3 r_1 \int d^3 r_2 w_{\mu'}(\mathbf{r}_1 - \mathbf{i}) w_{\nu'}(\mathbf{r}_2 - \mathbf{i}) V_p^m(\mathbf{r}_1 - \mathbf{r}_2) w_\mu(\mathbf{r}_1 - \mathbf{i}) w_\nu(\mathbf{r}_2 - \mathbf{i})$ can now be computed by separating the relative and center-of-mass coordinates. For deep lattices, the p -orbital Wannier functions are well approximated by the first excited states of harmonic oscillators (with the oscillator length ζ controlled by the lattice depth). The only non-zero interaction terms are the ones given in Eq. (1), with $V_1 = \frac{1}{4}(U_1 + U_{-1})$, $V_2 = \frac{1}{8}(U_1 + U_{-1} + 2U_0)$, and $V_3 = \frac{1}{8}(U_{-1} - U_1)$. Here, $U_m = 3\sqrt{2}R/(\sqrt{\pi}\zeta^5 M)$ defines the interaction strength in the scattering channel with angular momentum $m = 1, 0, -1$. A Zeemann splitting, which may be introduced by a magnetic field, leads to different detuning of the OFR laser for the three scattering channels. This makes the scattering length a_p^m dependent on m , and consequently the U_m 's can be different in magnitude and even in sign. Thus, the relative strengths and signs of $V_{1,2,3}$ can be varied by changing the strength of the Zeemann splitting together with the detuning of the OFR laser. By contrast, in a standard magnetic FR, $U_{-1} = U_{+1}$. In our case, breaking the symmetry between U_{-1} and U_{+1} leads to the orbital-changing term V_3 . Physically, it allows (p_x or p_y) particles to move on the two dimensional plane, instead of along a chain only. Since it explicitly breaks time-reversal symmetry (TRS), we can expect it to lead to novel phases reflecting that intriguing property.

Hamiltonian (1) generalizes the models of Refs. [17–22]. For $V_1 = V_2$, and $V_3 = 0$, it reduces to the SU(3) Hubbard model. One can visualize p -band fermions as particles carrying a color index representing the p_x , p_y , and p_z orbital states. Then, Hamiltonian (1) describes a three-color fermion model with color-dependent interaction, a novel color-changing term V_3 , and spatially anisotropic and color-dependent tunneling. We will show below that this model has a rich phase diagram with novel phases. Here, we focus on the strong-coupling limit for p -band filling 1/3, and determine the orbital order using a Gutzwiller mean-field ansatz.

In the strong-coupling limit,

$$|t_\parallel| \ll V_1, \quad |t_\parallel| \ll V_2 - V_3, \quad \text{and} \quad |t_\parallel| \ll V_2 + V_3, \quad (2)$$

double occupancy of the same site is suppressed. At 1/3 filling of the p -band, there is on average one p -band particle per site, and density fluctuations are frozen. Virtual hopping induces exchange interactions between nearest-neighbor orbitals (see Fig. 1). The situation bears some resemblance to the emergence of magnetic models, such

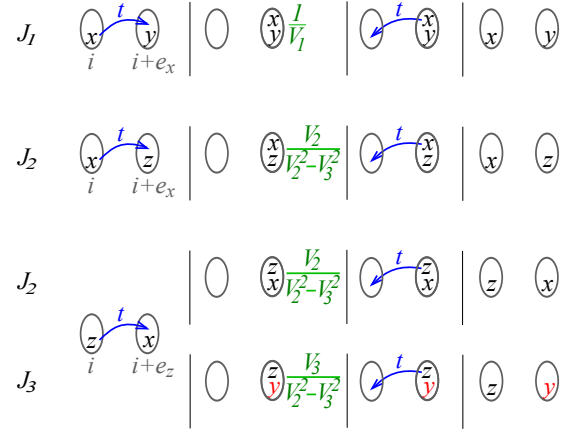


Figure 1: Sketch of the virtual hopping processes leading to the effective Hamiltonian (3). Neglecting t_\perp , these – plus the ones obtained by interchanging x and y – are the only ones. Note in particular the orbital-changing process J_3 . Gray ovals denote sites, the blue t tunneling processes, and the green fractions denote interactions. Orbitals p_μ are abbreviated as μ .

as the Heisenberg model, in the strong-coupling limit of the Hubbard model. The difference here is that three orbital (instead of two spin) states are involved. Since $|t_\perp| \ll |t_\parallel|$, perpendicular tunneling t_\perp can safely be neglected [19], and, for brevity, we write $t = t_\parallel$. Treating the tunneling t in (1) as a perturbation and following standard second-order perturbation theory, we obtain the effective Hamiltonian for 1/3 filling

$$H_{\text{eff}} = - \sum_{\mathbf{i}} \left[\sum_{\mu=x,y,z} \sum_{\delta=\pm \mathbf{e}_\mu} J_\mu n_{\mu, \mathbf{i}} (1 - n_{\mu, \mathbf{i}+\delta}) + \sum_{\mu=x,y} \sum_{\delta=\pm \mathbf{e}_\mu} (J_2 - J_1) n_{\mu, \mathbf{i}} n_{z, \mathbf{i}+\delta} - \sum_{\delta=\pm \mathbf{e}_z} J_3 (i c_{x, \mathbf{i}}^\dagger c_{y, \mathbf{i}} n_{z, \mathbf{i}+\delta} + h.c.) \right], \quad (3)$$

where we have used the constraint $n_{x, \mathbf{i}} + n_{y, \mathbf{i}} + n_{z, \mathbf{i}} = 1$, and defined $J_1 \equiv t^2/V_1$, $J_2 \equiv t^2 V_2/(V_2^2 - V_3^2)$, $J_3 \equiv t^2 V_3/(V_2^2 - V_3^2)$, and $J_x = J_y = J_1$, $J_z = J_2$. For $V_3 = 0$, $V_1 = V_2$, Eq. (3) reduces to $J_\mu n_{\mu, \mathbf{i}} n_{\mu, \mathbf{i}+\delta}$, a hallmark of the quantum 3-state Potts-like model [23].

To see which orbital order is favored, we first discuss the simple case of $J_3 = 0$. The first term of Eq. (3) always favors configurations where the orbitals at neighboring sites differ. (A) For $J_1 > \max(J_2, 0)$, both the first and second terms favor an alternating pattern between p_x - and p_y -particles in the xy -plane. (B) For $J_2 > \max(J_1, 0)$, the favored configuration is an alternating pattern between p_z and not- p_z . (C) For (the unstable case) $J_1, J_2 < 0$, the best configuration is a homogeneously filled lattice.

Certain aspects of Hamiltonian (3) become clearer when we rewrite it in terms of the generators of the SU(3) group. In terms of the Gell-Mann matrices $\lambda^{(i)}$

and the so-called F -spin operators $Y = \frac{1}{\sqrt{3}}c_\mu^\dagger \lambda_{\mu,\nu}^{(8)} c_\nu$ and $T^{(\alpha)} = \frac{1}{2}c_\mu^\dagger \lambda_{\mu,\nu}^{(\alpha)} c_\nu$ ($\alpha = 1, 2, 3$), H_{eff} becomes

$$H_{\text{eff}} = \frac{4}{3} \sum_i \left[(J_2 - J_1) Y_i - J_3 T_i^{(2)} \right] + 2 \sum_i \left[\sum_{\delta=e_x, e_y} (J_1 T_i^{(3)} T_{i+\delta}^{(3)} + \frac{2J_2 - J_1}{4} Y_i Y_{i+\delta} + \frac{J_2}{2} T_i^{(3)} Y_{i+\delta} + \frac{J_2}{2} Y_i T_{i+\delta}^{(3)}) \right. \\ \left. + J_2 Y_i Y_{i+e_z} + J_3 T_i^{(2)} Y_{i+e_z} + J_3 Y_i T_{i+e_z}^{(2)} \right], \quad (4)$$

where we neglected constant terms. In the basis (p_x, p_y, p_z) , Y and $T^{(3)}$ are diagonal, which means that terms such as $Y_i Y_j$, $Y_i T_j^{(3)}$, or $T_i^{(3)} T_j^{(3)}$ are Ising-like. The orbital-changing term V_3 leads to $T^{(2)} = \frac{1}{2i} (T^{(+)} - T^{(-)})$, where $T^{(\pm)}$ are ladder operators of the T -spin. $T^{(3)}$ and $T^{(2)}$ do not commute, but both commute with Y . This means that one can replace Y by its eigenvalues $-\frac{2}{3}$ (for $|p_z\rangle$) and $\frac{1}{3}$ (for $|p_x\rangle$ and $|p_y\rangle$), which gives some insight into the physics of Hamiltonian (4). Assuming that the ground state is bipartite with respect to the eigenvalue of Y [24], there are three different cases: (A) at all sites the eigenvalue of Y is $\frac{1}{3}$, (B) the eigenvalues $-\frac{2}{3}$ and $\frac{1}{3}$ alternate, and (C) all sites have eigenvalue $-\frac{2}{3}$. In the last case, there is one $|p_z\rangle$ -particle per site, whence there is no virtual tunneling, and the Hamiltonian vanishes. In the sectors A and B, it reads (neglecting constant terms)

$$H_{\text{eff}}^{(A)} = \frac{J_1}{2} \sum_i \sum_{\delta=e_x, e_y} \sigma_i^{(3)} \sigma_{i+\delta}^{(3)}; \quad (5a)$$

$$H_{\text{eff}}^{(B)} = -2J_3 \sum_{i \in \Omega} \sigma_i^{(2)}. \quad (5b)$$

Here, σ denotes the usual Pauli matrices, which act on the subspace spanned by $|p_x\rangle$ and $|p_y\rangle$. Sector A is reduced to the Ising model on decoupled xy -planes, which favors an antiferromagnetic ground state. This is just the model found in the 2D-case treated in [19, 20]. In sector B, Ω denotes the partition where Y has eigenvalue $\frac{1}{3}$. On these sites, J_3 acts as a magnetic field in the y -direction, lifting the degeneracy between $|p_x\rangle$ and $|p_y\rangle$ and leading to the ground state $(|p_x\rangle \pm i|p_y\rangle)/\sqrt{2}$ (for $J_3 \gtrless 0$).

Having obtained a qualitative picture of the expected phases, we now analyze the phase diagram of Hamiltonian (4) quantitatively. To this, we assume that correlations between sites are small so that the ground state can be approximated by a product over sites. To find the ground state of Hamiltonian (4), we employ the Gutzwiller variational wave function $|\Psi\rangle = \bigotimes_i (\cos \theta |p_x\rangle_i + \sin \theta \cos \phi |p_y\rangle_i + \sin \theta \sin \phi |p_z\rangle_i)$, which is a product over sites i , and minimize the energy of a cube with side length L (up to $L = 8$) under periodic boundary conditions. Note, however, that close to phase

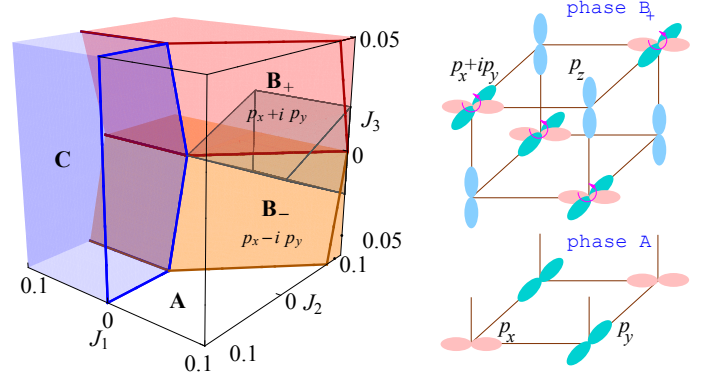


Figure 2: **Left:** The phase diagram of H_{eff} [Eq. (3)] at $1/3$ filling shows four phases: (A) antiferro-orbital order (empty region), (B₊) axial orbital order (red region, $J_3 > 0$) and similarly (B₋) (orange region, $J_3 < 0$), and finally (C) with tunneling completely frozen (blue region). The gray wedge indicates the region satisfying the strong-coupling conditions (2), $0 < J_{1,2} \ll 1$, $J_3 \ll J_2$. **Right:** sketch of phase B₊, in which $|p_z\rangle$ and $|p_x\rangle + i|p_y\rangle$ orbitals alternate, and phase A. Phase B₋ can be visualized from phase B₊ by replacing $|p_x\rangle + i|p_y\rangle$ with $|p_x\rangle - i|p_y\rangle$.

transitions, where fluctuations become important, such a mean-field ansatz is not valid.

The energy per site for even L is smaller than for odd L , showing that the ground state periodicity is indeed 2 [25]. In agreement with the qualitative picture above, we find three classes of ground states with different orbital order (summarized in Fig. 2): (A) For $J_1 > J_2 + |J_3|/2$ and $J_1 > 0$ we find an ‘antiferromagnetic phase’ similar to, *e.g.*, the 2D-model of Ref. [19]: in each xy -plane, sites with p_x - and p_y -orbitals alternate (similar to the antiferromagnetic Néel state). Since p_x - and p_y -particles do not tunnel in the z -direction, the xy -planes are decoupled, and within our approximation (*e.g.*, neglecting t_\perp), there is no long-range order in the z -direction. It is possible, however, that long-range order among the planes develops at low temperature for finite t_\perp . (B) For $J_1 < J_2 + |J_3|/2$ and $J_2 > -|J_3|/2$ the ground state shows *axial orbital order*. The state is bipartite with $|p_z\rangle$ on one sublattice and $(|p_x\rangle \pm i|p_y\rangle)/\sqrt{2}$ (for $J_3 \gtrless 0$, respectively) on the other sublattice (right-hand panel of Fig. 2). The degeneracy between $|p_x\rangle$ and $|p_y\rangle$ is lifted by a finite J_3 . The state $(|p_x\rangle \pm i|p_y\rangle)/\sqrt{2}$ has *finite angular momentum*, this novel phase breaks TRS [26]. (C) For $J_1 < 0$ and $J_2 < -|J_3|/2$ Pauli exclusion prohibits all tunneling t_\parallel (by filling $\alpha\beta$ -planes ($\alpha\beta = xy, xz, yz$) uniformly with p_α or p_β). This state is unstable, however, because it cannot fulfill the strong-coupling requirements (2). Interestingly, phases A and C preserve TRS, although V_3 in Hamiltonian (1) breaks it explicitly.

Experimentally, the different phases can, *e.g.*, be distinguished by measuring the density distribution after a time of flight t_{tof} . This relates to the in-trap momentum distribution via $\langle n(\mathbf{r}) \rangle_{t_{\text{tof}}} =$

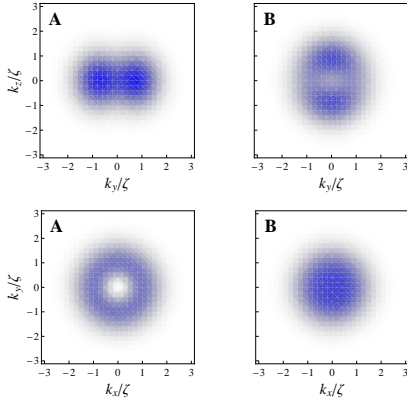


Figure 3: Predicted time-of-flight (TOF) density distributions, allowing to distinguish phases A and B in experiment. Lower (upper) row: $\langle n(\mathbf{r}) \rangle_{t_{\text{tof}}}$ integrated along z (x) in arbitrary scale. For example, when viewed along the z -direction, phase A displays a doughnut form (lower left panel) because of an incoherent addition of p_x - and p_y -Wannier envelopes. In phase B, the sites occupied by $(|p_x\rangle \pm i|p_y\rangle)/\sqrt{2}$ give a similar doughnut structure, but the hole at $k_x = k_y = 0$ is filled by the other half of the sites with p_z -particles. Similarly, viewing along the x -direction reveals the existence of p_z -particles in phase B, contrary to phase A (upper row).

$[M/(\hbar t_{\text{tof}})]^3 \sum_{\mu,\nu} w_{\mu}^*(\mathbf{k}) w_{\nu}(\mathbf{k}) \langle c_{\mu}^{\dagger}(\mathbf{k}) c_{\nu}(\mathbf{k}) \rangle$, with $w_{\mu}(\mathbf{k})$ the Fourier transform of the Wannier orbital $w_{\mu}(\mathbf{r})$, $c_{\mu}(\mathbf{k}) = \sum_{\mathbf{i}} e^{i\mathbf{k}\cdot\mathbf{i}} c_{\mu,\mathbf{i}}/L^{3/2}$, and $\mathbf{k} = M\mathbf{r}/(\hbar t_{\text{tof}})$. \mathbf{k} is \mathbf{k} modulo reciprocal lattice vectors. Features in the density distribution appear because of its non-trivial p -orbital Wannier envelope. This allows to distinguish phases A and B by their column density (*i.e.*, the density integrated along one spatial direction), see Fig. 3.

Observation of these novel phases requires that we simultaneously achieve strong interactions, $V \gg t$ and low temperatures $k_B T \ll t^2/V$, for the characteristic tunneling rate t and interaction energy V . At experimentally feasible temperatures, this requires a significant enhancement of the real part of the p -wave scattering volume via the OFR. In practice, however, this is limited by spontaneous emission, which broadens the resonance and also leads to recoil heating. For the example considered in [13]

based on the $^1S_0 \rightarrow ^3P_1$ intercombination line in ^{171}Yb , the atomic linewidth is ≈ 180 kHz, which limits the useful OFR p -wave enhancement. Other species such as ^{87}Sr , where the same transition has a linewidth of ≈ 7.5 kHz, should result in a substantial OFR, with a reasonable linewidth. Experimental studies of OFRs in related isotopes are currently underway [27].

In summary, we investigated the orbital order of spinless fermions in the p -band of a cubic lattice with interaction controlled by an OFR. The system can be realized with current technology. The model Hamiltonian can be expressed elegantly by Gell-Mann matrices. We analyzed the orbital order in the strong-coupling limit at p -band filling $1/3$ using a Gutzwiller-type ansatz. Besides a phase where all tunneling is blocked and an antiferro-orbital phase where p_x - and p_y -orbitals alternate, we found a novel phase with axial orbital order which not only breaks translational symmetry but also has macroscopic orbital angular momentum. We expect our results to stimulate future work on this subject. For example, it is interesting to investigate how quantum fluctuations affect the phase diagram: they might distort it [22] or even lead to disordered ‘orbital liquid’ states. Fluctuations are also expected to lift the degeneracy between p_x - and p_y orbitals at $J_3 = 0$, and possibly lead to *spontaneous* TRS breaking. Moreover, phase B_{\pm} may have interesting topological properties. For example, at an interface of two domains with $p_x + ip_y$ and $p_x - ip_y$ order, chiral zero mode fermions may arise. Finally, other lattices and the limit of small interactions, where related models show non-trivial color-superfluidity [17, 18, 21], are also interesting.

This work is supported in part by NSF Grant PHY05-51164. P. H. and M. L. acknowledge support by the Caixa Manresa, Spanish MICINN (FIS2008-00784 and Consolider QOIT), EU Projects AQUITE and NAMEQUAM, and ERC Grant QUAGATUA. E. Z. is supported by NIST Grant 70NANB7H6138 Am 001. W. V. L. is supported by ARO (W911NF-11-1-0230) and DARPA-OLE (ARO W911NF-07-1-0464). K. G. and I. H. D. are supported by NSF Grant PHY-0903953.

[1] Y. Tokura and N. Nagaosa, *Science* **288**, 462 (2000).
[2] P. Horsch, *Orbital Physics in Transition Metal Oxides: Magnetism and Optics. Handbook of Magnetism and Advanced Magnetic Materials* (2007).
[3] K. I. Kugel and D. I. Khomskii, *Sov. Phys. Usp.* **25**, 231 (1982).
[4] G. Khaliullin, *Prog. Theor. Phys. Suppl.* **160**, 155 (2005).
[5] A. Browaeys *et al.*, *Phys. Rev. A* **72**, 053605 (2005).
[6] M. Köhl *et al.*, *Phys. Rev. Lett.* **94**, 080403 (2005).
[7] T. Müller, S. Fölling, A. Widera, and I. Bloch, *Phys. Rev. Lett.* **99**, 200405 (2007).
[8] M. Anderlini *et al.*, *Nature* **448**, 452 (2007).
[9] G. Wirth, M. Ölschläger, and A. Hemmerich, *Nature*

Phys. **7**, 147 (2011).
[10] For an empty s -band, energy conservation can suppress undesired collisions $p + p \rightarrow s + d$ when using anharmonic on-site potentials created by optical superlattices.
[11] C. A. Regal, C. Ticknor, J. L. Bohn, and D. S. Jin, *Phys. Rev. Lett.* **90**, 053201 (2003).
[12] C. Chin, R. Grimm, P. Julienne, and E. Tiesinga, *Rev. Mod. Phys.* **82**, 1225 (2010).
[13] K. Goyal, I. Reichenbach, and I. Deutsch, *Phys. Rev. A* **82**, 062704 (2010).
[14] A. Isacsson and S. M. Girvin, *Phys. Rev. A* **72**, 053604 (2005).
[15] A. B. Kuklov, *Phys. Rev. Lett.* **97**, 110405 (2006).

- [16] W. V. Liu and C. Wu, *Phys. Rev. A* **74**, 013607 (2006).
- [17] A. Rapp, G. Zaránd, C. Honerkamp, and W. Hofstetter, *Phys. Rev. Lett.* **98**, 160405 (2007).
- [18] A. Rapp, W. Hofstetter, and G. Zaránd, *Phys. Rev. B* **77**, 144520 (2008).
- [19] E. Zhao, and W. V. Liu, *Phys. Rev. Lett.* **100**, 160403 (2008).
- [20] C. Wu, *Phys. Rev. Lett.* **100**, 200406 (2008).
- [21] S. Miyatake, K. Inaba, and S. Suga, *Physica C* **470**, S916 (2009).
- [22] T. A. Tóth, A. M. Läuchli, F. Mila, and K. Penc, *Phys. Rev. Lett.* **105**, 265301 (2010).
- [23] Orbital order in a simpler model without OFR, and its relation to the Potts model were discussed in the unpublished work of arXiv:0801.0888v1 by C. Wu.
- [24] In principle, more complex (*i.e.*, non-bipartite) partitions are possible, but the numerical mean-field analysis (see below) shows that these are the only relevant ones.
- [25] Further, we checked that for even L the occurring phases do not depend on L .
- [26] The derivation of (3) neglected repulsive off-site interactions $n_{\mu,i}n_{\mu,i+\delta}$, which for p -band fermions might be important compared to the exchange couplings J . However, the alternating occupations in the (physically relevant) phases A and B also minimize possible energy contributions from off-site repulsions. Hence, neglecting these is justified a posteriori.
- [27] S. Blatt *et al.*, *Phys. Rev. Lett.* **107**, 073202 (2011).